

Apoptosis in Caspase-inhibited Neurons

Christiane Volbracht,¹ Marcel Leist,¹ Stefan A. Kolb² and Pierluigi Nicotera¹

¹Department of Biology, Chair of Molecular Toxicology, University of Konstanz, Konstanz, Germany

²Laboratory for Electron Microscopy, Department of Pathology, University Hospital Zurich, Zurich, Switzerland

Accepted September 15, 2000.

Abstract

Background: There is growing evidence of apoptosis in neurodegenerative disease. However, it is still unclear whether the pathological manifestations observed in slow neurodegenerative diseases are due to neuronal loss or whether they are related to independent degenerative events in the axodendritic network. It also remains elusive whether a single, caspase-based executing system involving caspases is responsible for neuronal loss by apoptosis. **Materials and Methods:** Long-term exposure to the microtubule-disassembling agent, colchicine, was used to disrupt the axodendritic network and eventually trigger caspase-3-mediated apoptosis in cultures of cerebellar granule cells. For this model, we investigated the role of Bcl-2 and caspases in neurite degeneration and death of neuronal somata.

Results: Early degeneration of the axodendritic network occurred by a Bcl-2 and caspase-independent mechanism.

Conversely, apoptosis of the cell body was delayed by Bcl-2 and initially blocked by caspase inhibition. However, when caspase activity was entirely blocked by zVAD-fmk, colchicine-exposed neurons still underwent delayed cell death characterized by cytochrome c release, chromatin condensation to irregularly shaped clumps, DNA-fragmentation, and exposure of phosphatidylserine. Inhibitors of the proteasome reduced these caspase-independent apoptotic-like features of the neuronal soma.

Conclusion: Our data suggest that Bcl-2-dependent and caspase-mediated death programs account only partially for neurodegenerative changes in injured neurons. Blockage of the caspase execution machinery may only temporarily rescue damaged neurons and classical apoptotic features can still appear in caspase-inhibited neurons.

Introduction

Apoptosis is characterized by a conserved set of morphological changes, such as nuclear condensation and characteristic chromatin compaction (1,2). Apoptosis plays a physiological role in the functional development of the nervous system (3,4), but it also can underlie the accidental loss of neurons observed in cerebral ischemia and a plethora of chronic neurodegenerative diseases (5–7).

Despite the growing evidence that apoptosis takes part in neurodegenerative processes, it is still unclear whether the onset of symptoms and pathological manifestations are due to neuronal loss or, rather, to a preceding functional neuronal damage (8–10). A common early feature of neurodegenerative disorders is a disturbed intraneuronal trafficking and cytoskeletal alterations (11), often associated with formation of protein aggregates (12). It appears reasonable that, while these

events may be the cause of early manifestations of disease, apoptosis of the cell soma downstream to neurite dysfunction could be triggered subsequent to these events to dispose of dysfunctional neurons. Recent findings suggest that the pathogenesis of chronic neurodegenerative diseases, such as Alzheimer's or Huntington's disease, may be independent from neuronal loss, at least in early stages. For example, in transgenic mice overexpressing either a mutated huntingtin protein or amyloid precursor protein, neuronal dysfunction, such as motor alterations or deficits in synaptic activity, are observed prior to any major pathological evidence of death (13–15).

It is also unclear whether neuronal loss is dependent in all cases on the evolutionary-conserved apoptosis execution machinery, based on the type II subgroup of the family of caspases (16). Caspase inhibition affords significant protection in models of stroke (17,18) and pan-caspase inhibitors partially protect animals in models of neurodegeneration (19,20). On the other hand, caspase inhibition does not prevent cell death induced by radiation in hippocampal neurons (21), by DNA damage in cortical neurons (22), by potassium deprivation in cerebellar

Address correspondence and reprint requests to: Prof. P. Nicotera, Chair of Molecular Toxicology, Department of Biology, University of Konstanz, Box X911, 78457 Konstanz, Germany. Phone: +49-7531-884035; Fax: +49-7531-884033; E-mail: Pierluigi.Nicotera@uni-konstanz.de

granule cells (23), or by β -amyloid toxicity in telencephalic neurons (24).

Block of the apoptotic execution by caspase inhibitors may in many cases "buy time" for damaged neurons. These neurons could eventually recover in the presence of adequate trophic stimulation (25). However, inhibiting the caspase machinery may not block neuronal demise indefinitely and other death mechanisms may then be activated (26). Such caspase-independent cell death has been associated generally with necrosis (27) and in many cases this is the outcome in cultured cells (28). In neurons, caspase-dependent and -independent death pathways may coexist (29) and be activated locally, for example, at synaptic sites (30) or in neuronal somata (31).

We previously showed that disturbed cytoskeletal organization and neuronal trafficking by the microtubule poison colchicine caused apoptosis in cerebellar granule neurons (32). This occurred predominantly via caspase-3-dependent proteolysis (33). We also showed that block of apoptosis by caspase inhibitors or by energy deprivation suspended the execution of cell death, but did not affect degeneration of the neurite network (33). Here, we investigated whether neurite loss and death of the cell soma triggered by colchicine were modulated by the anti-apoptotic factor Bcl-2 and the final fate of caspase-inhibited neurons.

Materials and Methods

Materials

Calcein acetoxymethyl ester (calcein-AM), ethidium homodimer-1 (EH-1), H-33342, SYTOX, and tetramethylrhodamine ethylester (TMRE) were obtained from Molecular Probes (Eugene, OR). Pefabloc and the caspase substrates Ac-Asp-Glu-Val-aspartyl-(DEVD)-aminotrifluoromethyl coumarin (-afc) came from Biomol (Hamburg, Germany) Ac-Val-Asp-Val-Ala-aspartyl-(VDVAD)-afc from California Peptide Research (Napa, CA), and (+)-5-methyl-10,11-dihydro-5H-dibenzo[a,d]cyclohepten-5,10-imine (MK801) came from RBI (Biotrend Chemi kalien GmbH, Köln, Germany). The caspase inhibitor z-Val-Ala-DL-Asp-fluoromethylketone (zVAD-fmk), the calpain inhibitors Ac-Leu-Leu-L-norleucinal (LLN-CHO) and Ac-Leu-Leu-L-methional (LLM-CHO), the cathepsin B inhibitor z-Phe-Lys-2,4,6-trimethylbenzoyloxymethyl ketone (zFK-tmk) and amino acid ketone z-Phe-chloromethylketone (zF-cmk) were obtained from Bachem Biochemica GmbH (Heidelberg, Germany). The proteasome inhibitor *clasto*-lactacystin β -lactone was from Calbiochem-Novabiochem (Bad Soden, Germany) and the inhibitor for cathepsin B CA-074 Me (CA074) was from Peptide Institute (Osaka, Japan). AlexaTM568-labeled annexin V (annexin V) was from Boehringer-Mannheim (Mannheim, Germany). Solvents and inorganic salts were from Merck (Darmstadt, Germany) or Riedel-de Haen (Seelze, Germany). All other reagents not

further specified were from Sigma (Deisenhofen, Germany).

Animals

Bcl-2 overexpressing mice (34) or corresponding wild-type animals were generously provided by Dr. J.-C. Martinou (Serono Pharmaceuticals, Geneva, Switzerland). All animals used for cell preparations were genotyped by polymerase chain reaction (PCR). For other experiments, 8-day-old specific pathogen free BALB/c mice were obtained from the Animal Unit of the University of Konstanz. All experiments were performed in accordance with international guidelines to minimize pain and discomfort (National Institutes of Health-Guidelines and European Community Council Directive 86/609/EEC).

Cell Culture

Murine cerebellar granule neurons (CGC) were isolated and cultured as described previously (33). Dissociated neurons were plated on 100 μ g/ml (250 μ g/ml for glass surfaces) poly-L-lysine (MW > 300 kDa) coated dishes at a density of about 0.25×10^6 cells/cm² (800,000 cells/ml; 500 μ l/well, 24-well plate) and cultured in Eagle's Basal Medium (BME; Gibco, Eggenstein, Germany) supplemented with 10% heat-inactivated fetal calf serum (FCS), 20 mM KCl, 2 mM L-glutamine, and penicillin-streptomycin. Cytosine arabinoside (10 μ M) was added 48 hr after plating. Neurons were used without further medium changes after 5 days *in vitro* (DIV). The cultures were exposed to colchicine in their original medium for all experiments in the presence of 2 μ M MK801 and 2 mM Mg²⁺ to prevent N-methyl-D-aspartate receptor activation, and 10 mM glucose to prevent energy depletion and excitotoxicity (33). All inhibitors were added 30 min before colchicine, unless stated otherwise.

Viability Assays

To assess plasma membrane integrity and nuclear morphology, CGC were loaded with 0.5 μ M calcein-AM for 5 min (cells with intact membranes displayed green fluorescence) in the presence of 1 μ M EH-1 (cells with broken membranes exhibit red fluorescent chromatin stain) and 1 μ g/ml H-33342 (cell permeable, blue fluorescent chromatin stain). Alternatively, double-staining of neuronal cultures was performed with 0.5 μ M SYTOX (nonmembrane permeable, green fluorescent chromatin stain) and 1 μ g/ml H-33342. Cell death was characterized by scoring condensed and highly fluorescent nuclei. About 600–1000 cells were counted in five different fields in two to three different culture wells, and experiments were repeated in at least three different preparations.

Mitochondrial Function and Integrity

The mitochondrial membrane potential ($\Delta\Psi$) was monitored in cells loaded with the fluorescent

indicator TMRE (5 nM, $\lambda_{\text{ex}} = 568 \text{ nm}$, $\lambda_{\text{em}} = 590 \text{ nm}$) for 10 min. Fluorescent intensity was normalized to that of untreated control neurons, which was set to 100%. The fluorescence of neurons treated with the mitochondrial poison carbonyl cyanide chlorophenylhydrazone (CCCP, 20 μM) was used as reference for depolarized mitochondria (35). The release of cytochrome c from mitochondria was analyzed by immunocytochemistry of CGC grown on glass-bottomed culture dishes. After the experiment, CGC were fixed with 4% paraformaldehyde and permeabilized with 0.1% Triton X-100 in phosphate-buffered saline (PBS). To monitor cytochrome c redistribution in apoptosis, neurons were stained with a monoclonal antibody directed against the native cytochrome c (1:300, clone 6H2.B4; Pharmingen, San Diego, CA). As secondary antibody, we used an AlexaTM ($\lambda_{\text{ex}} = 488 \text{ nm}$, $\lambda_{\text{em}} = 512 \text{ nm}$)-coupled anti mouse antibody (1:300; Molecular Probes, Eugene, OR). For analysis by confocal microscopy (TCS-4D UV/VIS confocal scanning system, Leica AG, Benzheim and Leica Lasertechnik, Heidelberg, Germany), CGC were embedded in PBS containing 50% glycerol and 0.5 $\mu\text{g/ml}$ H-33342. Alternatively, the release of cytochrome c from mitochondria was analyzed by selective digitonin permeabilization, as described previously (35,36), with the following modifications: at the indicated time points, the culture medium was exchanged for permeabilization buffer [210 mM D-mannitol, 70 mM sucrose, 10 mM N-2-hydroxyethylpiperazin-N'-2-ethansulfonic acid (HEPES), 5 mM succinate, 0.2 mM ethylenglycol-bis(β -aminoethylether)-N,N,N',N'-tetraacetic acid (EGTA), 0.15% bovine serum albumin, 75 $\mu\text{g/ml}$ digitonin, pH 7.2]. Then, cell culture plates were gently shaken for 10 min at 4°C, before removing the permeabilization buffer, which contained the cytosolic fraction, and adding 0.3% Triton X-100 in PBS for 10 min at 4°C to release residual cytochrome c, which was retained within the organelle fraction. Samples were centrifuged for 10 min at 13000 \times g and protein from the supernatant of the centrifugation of the cytosolic and the organelle fraction was precipitated with 10% trichloroacetic acid and separated on a 12% polyacrylamide gel. All samples were obtained from cell culture dishes (12 well) containing 10⁶ cells per well. Cytochrome c was detected with a monoclonal antibody raised against pigeon cytochrome c (1.5 $\mu\text{g/ml}$, clone 7H8.2C12; Pharmingen, San Diego, CA) after blotting on nitrocellulose membranes. At the digitonin concentration used in the experiments, >90% neurons released lactate dehydrogenase and became permeable to the fluorescent chromatin dye SYTOX. Control experiments showed that cytochrome c was not released into the supernatant of untreated cultures, even after 20 min incubation in permeabilization buffer. Treatment of these cultures with Triton X-100 led to a maximal release of cytochrome c into the supernatant.

Transmission Electron Microscopy

Neurons were cultured on chamber slides (LabTek, Nalge Nunc International, Naperville, IL), fixed by addition of 2.5% glutaraldehyde (in phosphate buffer, 0.1 M, pH 7.4) and stored in fixative for 2–3 days prior to further processing. Specimens then were washed in phosphate buffer, postfixed with 1% osmium tetroxide and dehydrated in graded alcohol. Thereafter, BEEMTM capsules (Electron Microscopy Sciences, Fort Washington, PA) were filled with Epon resin and put on the slides for embedding of the cells. Epon was polymerized at 60°C and BEEMTM capsules were detached from the glass slides in liquid nitrogen. Ultrathin sections (60–80 nm) were cut on a Reichert ultramicrotome and contrasted with uranyl acetate and lead citrate. Stained sections were observed and photographed in a Philips CM 10 electron microscope operating at 80 kV.

Visualization of Phosphatidylserine Translocation

Surface phosphatidylserine (PS) expression was analyzed by annexin V staining and confocal microscopy as described previously (37). Briefly, 10 min before the incubation periods, CGC were stained with calcein-AM and H-33342 to visualize plasma membrane integrity and chromatin structure. Then, CGC were washed for 10 sec with binding buffer (10 mM HEPES, 140 mM NaCl, 2.5 mM CaCl₂, 10 mM MgCl₂, pH 7.4) and subsequently incubated for 2 min in the dark with AlexaTM568-labeled annexin V diluted 1:100 in binding buffer. After a new wash with binding buffer, stained live cultures were immersed in binding buffer (4°C) and visualized by three channel confocal microscopy (blue, chromatin structure; green, membrane integrity; red, annexin binding) using a 63 \times /NA 1.32 UV-corrected lens.

Enzymatic Assays

The enzymatic activities of recombinant murine caspase-2, generously provided by Dr. P. Vandenabeele (38), and recombinant caspase-3, generously provided by Dr. F.O. Fackelmayer (39), were assayed using continuous fluorometric assays analogous to those described before (40–42). Caspase-2 activity measurements were performed with 100 μM of the peptide substrate VDAD-afc (41) in reaction buffer (50 mM HEPES, 1% sucrose, 0.1% 3-[(3-cloamidopropyl)-dimethylammonio]-propanesulfate (CHAPS), 10 mM dithiothreitol) at pH 6.8 (43). The activity of caspase-3 was determined in reaction buffer pH 7.4 with the peptide substrate DEVD-afc (100 μM). Briefly, appropriate dilutions of enzyme were added to various concentrations of inhibitor and incubated for 10 min at room temperature. The enzymatic reaction was started in a final volume of 100 μl by adding reaction buffer containing the substrate. Release of afc was monitored over a time period of 30 min at 37°C in microtiter plates at $\lambda_{\text{ex}} = 400 \text{ nm}$ and $\lambda_{\text{em}} = 508 \text{ nm}$. The activity was calibrated with

afc standard solutions and the formation of 1 pmol afc/min was defined as one micro unit (μ U). In neurons, caspase-activity (measured by DEVD-afc cleavage for caspase-3-like activity and VDVAD-afc for caspase-2-like activity) was measured as described previously (40). Neurons were lysed in 25 mM HEPES, 5 mM $MgCl_2$, 1 mM EGTA, 0.5% Triton X-100, 1 μ g/ml leupeptin, 1 μ g/ml pepstatin, 1 μ g/ml aprotinin, 1 mM Pefabloc, pH 7.5. The fluorometric assay was performed with a total protein amount of 5 μ g and substrate concentration of 50 μ M (DEVD-afc) or 100 μ M (VDVAD-afc). Release of afc was followed continuously in reaction buffer (pH 7.5 for DEVD-afc or pH 6.8 for VDVAD-afc) over a time period of 30 min at 37°C. Measurement of adenosintriphosphate (ATP) was performed luminometrically after lysing cells in ATP-releasing agent (Sigma) with a commercial kit (Boehringer-Mannheim) as described earlier (28,35).

Electrophoretic Assay

Field inversion gel electrophoresis was performed as described previously (35,37). About 5×10^6 cells (corresponding to 6 wells of a 12 well plate) were embedded into 40 μ l agarose blocks. λ deoxyribonucleic acid (DNA) concatemers [$n \times 50$ kilo base pairs (kbp)] were used as molecular weight markers.

Statistics

Experiments to determine cell viability, mitochondrial function, or caspase activities were run as triplicates and repeated in three to five cell preparations. Statistical significance was calculated on the original data sets using the Student's *t*-test. When variances within the compared groups were not homogeneous, the Welch test was applied. Western blots, field inversion gel electrophoresis, and transmission electron microscopy analysis were performed with samples from at least three independent cell preparations.

Results

Delayed Cell Death in the Presence of Bcl-2 or the Caspase Inhibitor zVAD-fmk

Neuronal death due to the microtubule-depolymerizing agent colchicine is characterized by an initial disruption of the axodendritic network followed by apoptotic nuclear condensation. In agreement with previous observations (33), treatment with the caspase inhibitor zVAD-fmk (100 μ M) prevented colchicine-induced nuclear alterations and protected neuronal somata from cell death for 18–24 hr. However, the microtubule breakdown still occurred and the majority of the neurite network was lost (Fig. 1A). After prolonged exposure of CGC to colchicine plus zVAD-fmk (28–36 hr), nuclei started condensing (Fig. 1A, right panel), and the frequency of cells with condensed chromatin reached a maximum of nearly 90% after 60 hr (Fig. 1C). Treatment with 100 μ M zVAD-fmk alone did not affect neuronal viability or

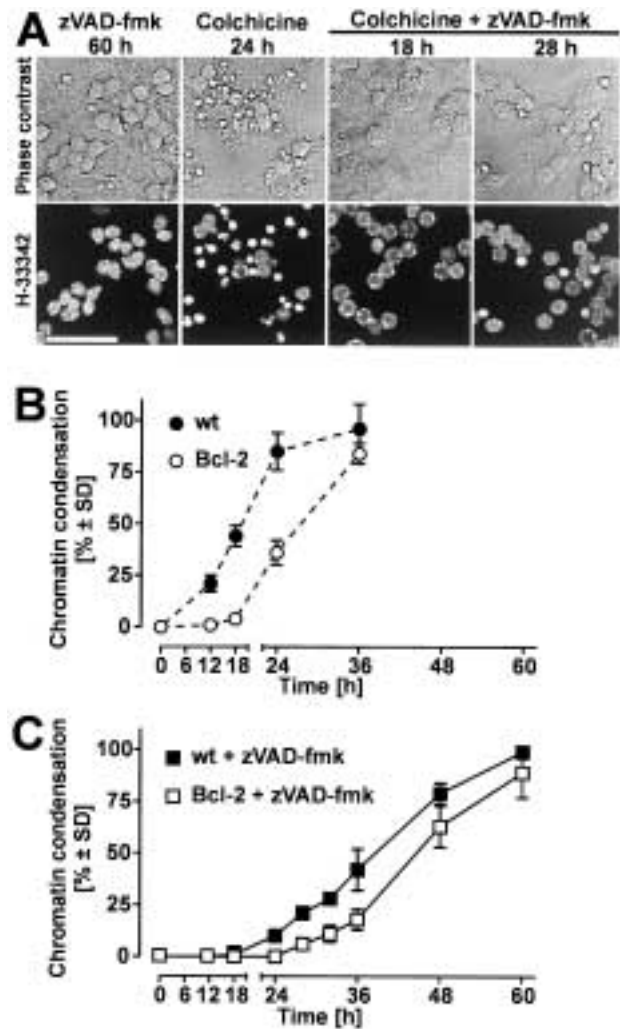


Fig. 1. Caspase-inhibited neurons undergo delayed chromatin condensation and cell death. (A) Neurons were treated with colchicine (1 μ M) in the presence or absence of N-benzyloxycarbonyl-Val-Ala-aspartyl-fluoromethyl ketone (zVAD-fmk; 100 μ M), or with zVAD-fmk alone. At the indicated time points, nuclei were stained with H-33342. Then, phase contrast and chromatin fluorescence were imaged simultaneously by confocal microscopy (63 \times , NA 1.32 lens). The width of the scale bar corresponds to 40 μ m. Cultures from wild-type mice (wt) or Bcl-2-overexpressing mice (Bcl-2) were treated with colchicine alone (B) or with colchicine plus zVAD-fmk (C). At the time points indicated, cultures were stained with H-33342, and the percentage of nuclei with condensed chromatin was counted. Data are means \pm standard deviation (SD) from seven determinations.

morphology and did not elicit visible changes in chromatin structure for at least 60 hr (Fig. 1A, left panel).

The oncogene, Bcl-2, has been suggested as a guardian of microtubule integrity (44) and it is a potent anti-apoptotic factor (45). Therefore, we investigated whether the initial colchicine-induced microtubule breakdown or subsequent nuclear condensation would be modulated by Bcl-2. First, experiments were performed in CGC cultures from Bcl-2-overex-

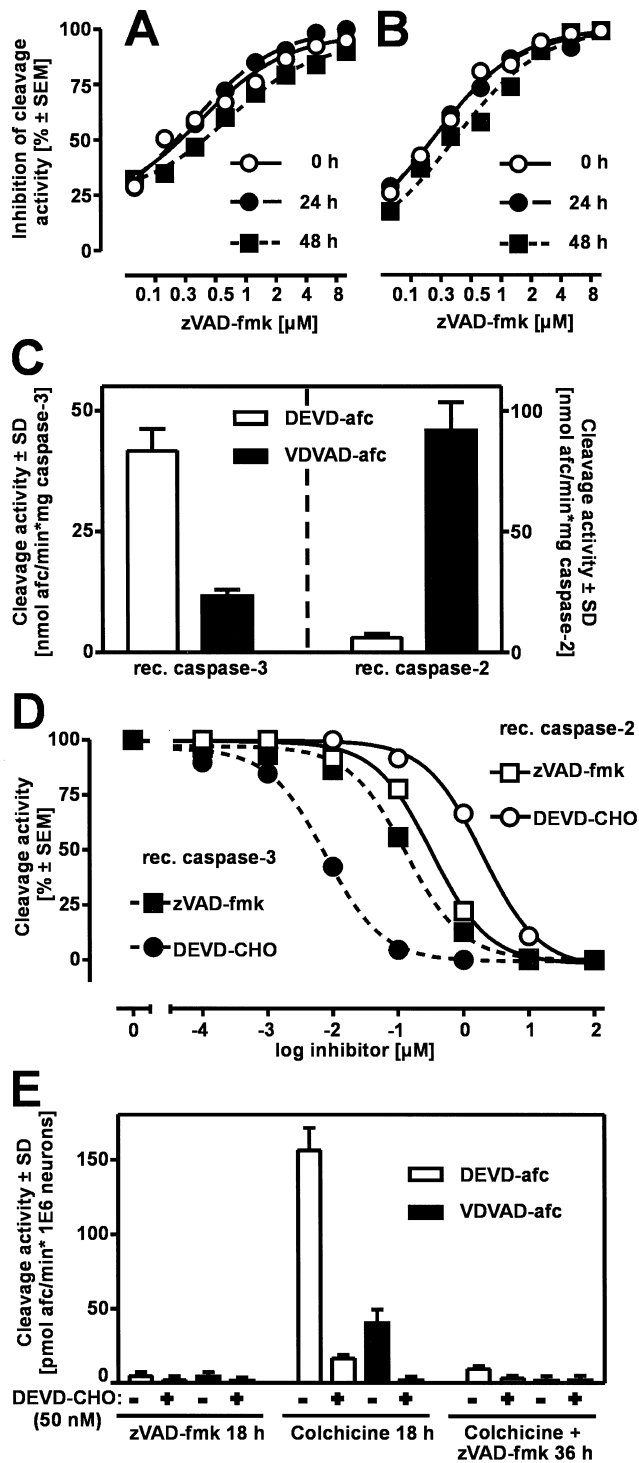


Fig. 2. Caspase inhibitor zVAD-fmk is stable and prevents caspase activity. Medium alone (A) or neuronal cultures (B) were supplemented with N-benzyloxycarbonyl-Val-Ala-aspartyl-fluoromethyl ketone (zVAD-fmk; 100 μ M). After the indicated time points, supernatant was removed and incubated in different dilutions with recombinant caspase-3 (30 ng/ml). Then, caspase-3 activity was measured by Ac-Asp-Glu-Val-aspartyl-aminotrifluoromethyl coumarin (DEVD-afc) cleavage. Data are means from five determinations. Error bars are smaller than the data symbols. (C) Enzymatic activities of recombinant caspase-2 and caspase-3 (0.6 μ g/ml) were measured with the

pressing mice exposed to colchicine alone. Microtubule breakdown was not altered significantly by Bcl-2 overexpression (data not shown). However, caspase activation, measured 10 hr after exposure to colchicine was entirely blocked. This inhibition was ephemeral, since caspase activity then increased to an extent similar to that found in cultures from wild type (wt) animals, with a delay of 10 hr (data not shown). Similar to the delay in caspase activation, Bcl-2 caused a transient (10 hr) protection from chromatin condensation (Two-way ANOVA, group-interaction; $p < 0.0001$), but did not alter the ultimate extent of death after 36 hr (Fig. 1B). The caspase-independent death triggered by colchicine in the presence of zVAD-fmk also was delayed by Bcl-2 in a similar way (Fig. 1C, Two-way ANOVA; $p < 0.0001$). These findings are in agreement with a recent study where inhibition of the execution caspases was achieved using cells from apaf-1 knockout (46) and suggested that both caspase-dependent and -independent types of cell death were modulated by Bcl-2.

Kinetics and Extent of Caspase Inhibition by zVAD-fmk

For our studies on caspase-independent neuronal death, we used the demethylated form of zVAD-fmk, which may be relatively unstable in certain organic buffers in vitro (47). Therefore, we tested the chemical stability of zVAD-fmk in the cell culture medium used for our experiments. Medium alone or medium from neuronal cultures was supplemented with zVAD-fmk and samples were collected after different time points (0–48 hr) to determine their inhibitory potency towards recombinant caspase-3. When tested in serial dilutions, all medium samples inhibited enzymatic activity of recombinant caspase-3 to a similar extent (Figs. 2A and B). The calculated half life of zVAD-fmk was >48 hr in both neuronal culture medium and medium from neuronal cultures. These findings suggested that zVAD-fmk was a useful tool to suppress caspase-dependent apoptosis after long-term incubation at 37°C.

Although zVAD-fmk often has been used as a pan-caspase inhibitor, the inactivation rate for dif-



peptide substrates DEVD-afc and Ac-Val-Asp-Val-aspartyl-aminotrifluoromethyl coumarin (VDVAD-afc). Data are means \pm standard deviation (SD) from three measurements. (D) Ac-Asp-Glu-Val-Asp-aldehyde (DEVD-CHO) and zVAD-fmk in concentration from 0.1 nM to 100 μ M were incubated with recombinant caspase-2 (15 ng/ml) or caspase-3 (30 ng/ml). Then, enzymatic activity for caspase-2 (VDVAD-afc) and caspase-3 (DEVD-afc) was determined. Data are means from six determinations. Error bars are smaller than the data symbols. (E) Neurons were treated with colchicine (1 μ M) in the presence or absence of zVAD-fmk (100 μ M) or with zVAD-fmk alone. After the indicated time points, cells were lysed and lysates were incubated in vitro in the presence or absence of DEVD-CHO (50 nM) for 5 min at room temperature. Then, cleavage activity was measured with the substrates DEVD-afc and VDVAD-afc. Data are means \pm SD from three experiments.

ferent caspase isoenzymes varies greatly (47). In some experimental systems caspase-2 in particular, appeared to be inactivated at a considerably slower rate than all other caspases (47). Since caspase-2 may have a role in neuronal apoptosis (25,48), we evaluated the inhibitory potency of zVAD-fmk for recombinant murine caspase-2, compared with caspase-3 under various conditions. The specific enzyme activities of recombinant caspase-2 and -3 were determined with the peptide substrates VD-VAD-afc and DEVD-afc (Fig. 2C). Caspase-2 cleaved VD-VAD-afc with a very high specific activity; whereas, it was 15 times less efficient at cleaving DEVD-afc. In contrast, caspase-3 cleaved both DEVD-afc and VD-VAD-afc with high activity (Fig. 2C). For inhibition experiments, the enzymes were then used at optimal conditions, such as with DEVD-afc as caspase-3 substrate and VD-VAD-afc as caspase-2 substrate. The irreversible caspase inhibitor, zVAD-fmk, blocked activity of both caspase-3 and -2 within a similar range of potency. The concentrations calculated to produce half-maximal inhibition within our experimental setup (preincubation of the enzyme for 10 min) were $0.15 \mu\text{M}$ for caspase-3 and $0.4 \mu\text{M}$ for caspase-2 (Fig. 2D). As reference, we used a reversible peptide inhibitor, the aldehyde DEVD-CHO, for which the IC_{50} can be accurately calculated. This peptide is highly specific for caspase-3 ($\text{IC}_{50} = 4 \text{ nM}$ in our system), compared with caspase-2 ($\text{IC}_{50} = 2000 \text{ nM}$). We did not observe a detectable influence of different pH (6.8, 7.2, and 7.4) on the inhibitory effects of both peptides on caspase-2 activity (data not shown). Finally, we determined whether caspase-2 activation occurred during colchicine-induced apoptosis. Therefore, we measured DEVD-afc and VD-VAD-afc cleavage in the presence or absence of the peptide aldehyde DEVD-CHO in neuronal lysates (Fig. 2E). We used a concentration of DEVD-CHO (50 nM) that inhibited caspase-3, but not caspase-2, activity (Fig. 2D). Both DEVD-afc and VD-VAD-afc were cleaved in neurons treated with colchicine alone. In the presence of DEVD-CHO, cleavage activity for both DEVD-afc and VD-VAD-afc was substantially reduced, which strongly suggested that the VD-VAD-afc cleavage activity was not due to caspase-2, but most likely to caspase-3 ability to degrade VD-VAD-afc. During colchicine-induced delayed cell death (i.e., in presence of zVAD-fmk), we did not detect any activity of the execution caspases measured by either DEVD-afc or VD-VAD-afc cleavage (Fig. 2E). Altogether, these data suggested that zVAD-fmk inhibited permanently and completely neuronal execution caspases relevant for colchicine toxicity.

Colchicine-induced Apoptotic Chromatin Changes in the Presence of zVAD-fmk

The alterations of nuclear morphology in colchicine-treated neurons were examined by transmission electron microscopy (Fig. 3). Control neurons had

oval-shaped nuclei characterized by an overall loose chromatin structure containing some dense spots. When neurons were treated with colchicine, nuclei shrank and the chromatin condensed near the nuclear periphery to crescent-shaped cap-like structures. At later stages, aggregated chromatin was fragmented into globular structures, and the cytoplasm condensed. At that time (16–18 hr), neurons

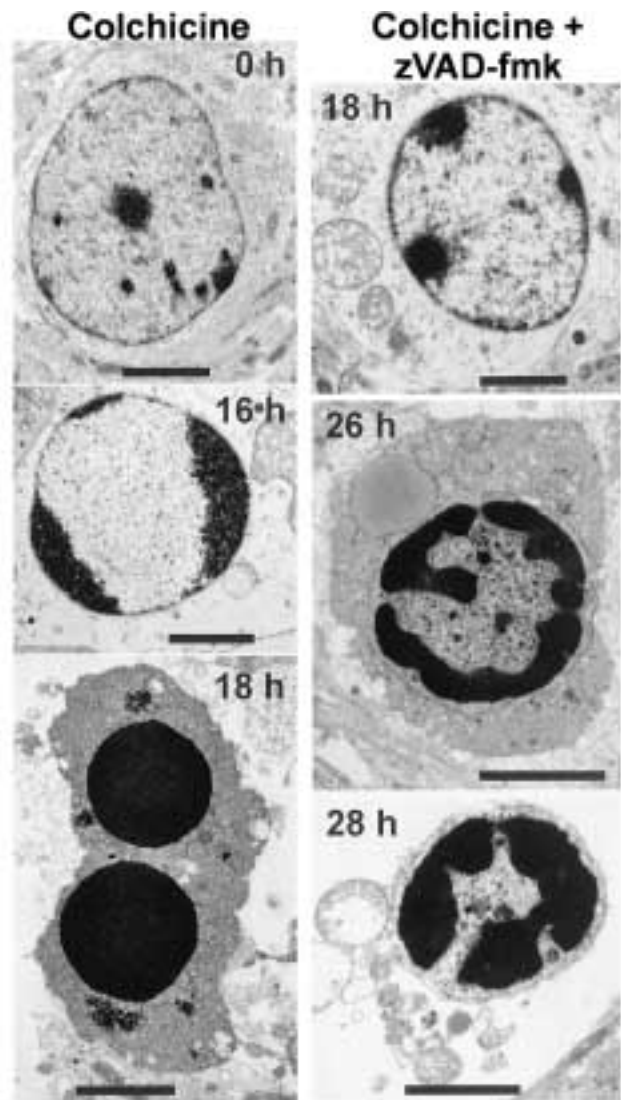


Fig. 3. Nuclei of caspase-inhibited neurons display apoptotic morphological changes. Neurons were treated with colchicine ($1 \mu\text{M}$) in the absence (left panel) or presence (right panel) of N-benzyloxycarbonyl-Val-Ala-aspartyl-fluoromethyl ketone (zVAD-fmk; $100 \mu\text{M}$). At different time points, cultures were fixed with 2.5% glutaraldehyde for transmission electron microscopy analysis. In colchicine-treated neurons, chromatin condensed to crescent- and sphere-shaped structures. Early stages (18 hr) of chromatin condensation in caspase-inhibited neurons were characterized by compaction of DNA under the nuclear envelope. At later time points ($>24 \text{ hr}$), lumpy, highly condensed chromatin structures were formed. The width of scale bars corresponds to $2 \mu\text{m}$.

exposed to colchicine plus zVAD-fmk displayed only slight changes of chromatin, which appeared lumpier and started clustering near the nuclear envelope. Later (after 26–28 hr), the chromatin of neurons treated with colchicine plus zVAD-fmk strongly condensed to irregularly shaped masses under the nuclear envelope. In parallel, the cytoplasm appeared more condensed.

To examine whether the apoptotic-like morphological changes in zVAD-fmk-inhibited neurons were paralleled by DNA-damage, we measured DNA-fragmentation (Fig. 4). High molecular weight DNA-fragments (600, 300 and 50 kbp) formed in CGC treated with colchicine regardless of the presence or absence of zVAD-fmk. Occurrence of DNA-fragmentation paralleled the onset of nuclear condensation in time and was quantitatively similar to that triggered by colchicine alone. Staining of cells with fluorescent dyes indicated that the majority of neurons had an intact plasma membrane when DNA-fragmentation started. At late time point (36 hr), an increasing number of neurons (about 20%)

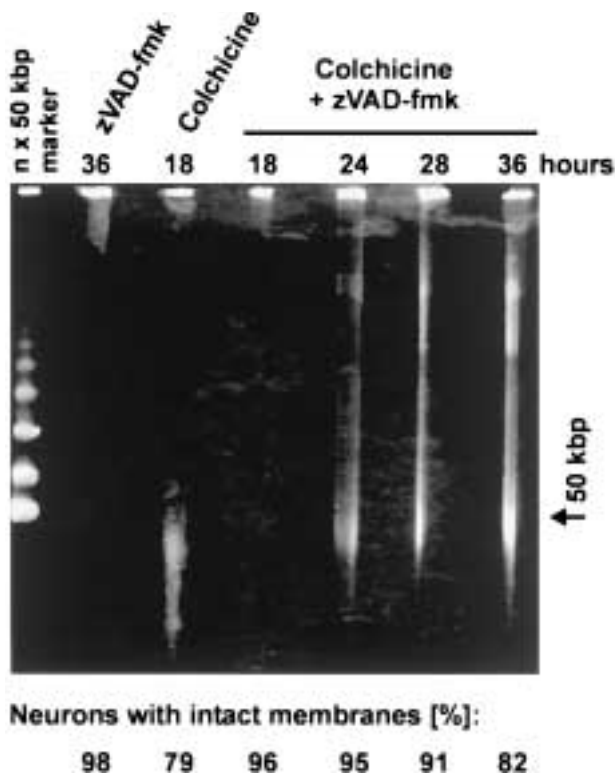


Fig. 4. Caspase-inhibited neurons display chromatin degradation. Neurons were incubated with colchicine ($1 \mu\text{M}$) in the presence or absence of N-benzyloxycarbonyl-Val-Ala-aspartyl-fluoromethyl ketone (zVAD-fmk; $100 \mu\text{M}$) or with zVAD-fmk alone. After different time points, the percentage of neurons retaining plasma membrane integrity was determined by counting calcein acetoxymethyl ester (calcein-AM)-positive cells. Then, DNA fragmentation was analyzed by field-inversion gel electrophoresis. The arrow indicates high molecular weight DNA fragments of 50 kbp.

underwent secondary lysis, consistent with the ultrastructural finding that nuclear changes were followed by a loss of plasma membrane integrity.

Colchicine-induced PS Translocation in the Presence of zVAD-fmk

Translocation of PS from the inner to the outer layer of the plasma membrane is an early event in neurons undergoing apoptosis (37), for example, those treated with colchicine alone (33). Surface PS was analyzed by staining live neurons with fluorescent-labeled annexin V. Neurons, exposed to colchicine plus zVAD-fmk for 24 hr, appeared to have intact plasma membranes, as indicated by the calcein-AM staining (Fig. 5, left panel). At 24 hr, about 10% of the neurons displayed nuclei with the characteristic mottled type of chromatin condensation (Fig. 5, indicated by arrows, middle panel). Nearly 50% of

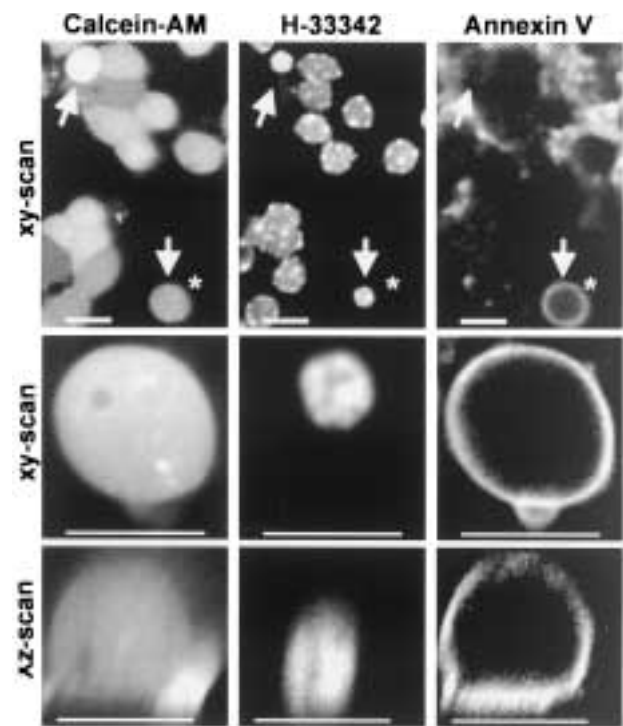


Fig. 5. Caspase-inhibited neurons display PS-translocation. Neurons were incubated with colchicine ($1 \mu\text{M}$) and N-benzyloxycarbonyl-Val-Ala-aspartyl-fluoromethyl ketone (zVAD-fmk; $100 \mu\text{M}$) for 24 hr and stained with fluorescent annexin V [phosphatidylserine (PS)-translocation], calcein acetoxymethyl ester (calcein-AM; plasma membrane integrity) and H-33342 (chromatin structure). Fluorescence images were collected by confocal microscopy ($63\times$, NA 1.32 lens). Top: xy-section through the cell bodies. Arrows indicate condensed nuclei and an asterisk indicates an annexin V-positive neuron. The width of the scale bar corresponds to $10 \mu\text{m}$. Middle: xy-section through the annexin V-positive neuron in higher magnification. Bottom: transversal section (xz-plane) demonstrates that the entire surface of the neuron was surface stained with annexin V. The width of the scale bar corresponds to $9 \mu\text{m}$. Data are representative of five experiments in three independent cell preparations.

neurons with condensed nuclei and intact plasma membranes displayed PS exposure (Fig. 5, indicated by an asterisk, left panel), and this percentage of annexin-positive neurons remained constant at later stages. PS was localized on the surface of the neurons and entirely surrounded the cell bodies (middle and lower rows).

Rupture of Outer Mitochondrial Membrane and Cytochrome c Release in Colchicine-induced Apoptosis in the Presence of zVAD-fmk

To investigate whether mitochondria underwent apoptotic-like changes also in caspase-inhibited neurons, we measured mitochondrial membrane potential ($\Delta\Psi$) using the mitochondrial potential-sensitive dye TMRE. In CGC exposed to colchicine alone, TMRE fluorescence dropped by about 20% after 12 hr, further declined to about 30% of control after 18 hr, and was completely lost after 24 hr. In the presence of zVAD-fmk, loss of $\Delta\Psi$ started with a delay of 8 hr, and was completed after 32 hr. The loss of $\Delta\Psi$ was paralleled by a 90% decline of the intracellular ATP levels in both colchicine- and colchicine plus zVAD-fmk-treated neurons (not shown). We investigated whether those changes in mitochondrial membrane potential also were reflected by ultrastructural alterations of the mitochondria (Fig. 6A). Mitochondria from control neurons (colchicine 0 hr) appeared elongated and oval-shaped, with dense cristae. Mitochondria from colchicine-treated neurons (colchicine 16 hr) were enlarged frequently, often up to double of their original size. Observed alterations included the formation of large blebs and the rupture of the outer mitochondrial membrane. Similar changes were observed in mitochondria from colchicine-treated neurons in the presence of zVAD-fmk (colchicine plus zVAD-fmk, 16 hr). These findings suggested that colchicine-induced microtubule depolymerization somehow triggered irreversible mitochondrial alterations, and these may have committed neurons to death, in the presence or absence of caspase activation.

In order to obtain a quantitative overall measure of mitochondrial membrane rupture in the neuronal population, we characterized the release of cytochrome c from mitochondria to the cytoplasm (Figs. 6B and C). In control neurons (colchicine 0 hr), immunoreactive cytochrome c formed a punctate pattern in the neurite structures and around the nuclei. The structures stained by anti-cytochrome c colocalized with the mitochondrial marker, Mitotracker Red (not shown). 30% of the neurons exposed to colchicine for 12 hr displayed a diffuse cytosolic cytochrome c pattern and nuclear localization of cytochrome c. 80% of these latter cells had a condensed apoptotic nucleus (Figs. 6B and C, middle left panel). The diffuse cytosolic cytochrome c pattern was also observed in some neurons that still displayed normally shaped nuclei, indicating that cytochrome c release preceded nuclear condensation. Some of the neurons with clearly condensed nu-

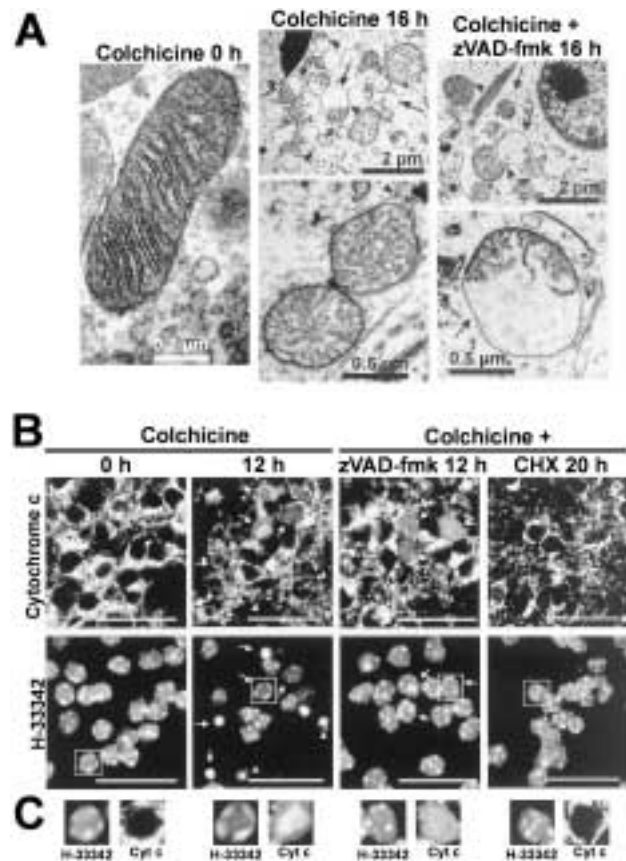


Fig. 6. Mitochondrial damage and cytochrome c translocation caused by colchicine is not prevented by zVAD-fmk.

(A) Neurons were treated with colchicine (1 μ M) in the absence or presence of N-benzyloxycarbonyl-Val-Ala-aspartyl-fluoromethyl ketone (zVAD-fmk; 100 μ M). After 16 hr, cells were fixed with 2.5% glutaraldehyde for transmission electron microscopy analysis. Arrows indicate blebbing of mitochondria, and arrowheads indicate rupture of the outer mitochondrial membrane. Neurons were exposed to colchicine (1 μ M), either directly, or in the presence of zVAD-fmk (100 μ M), or in the presence of cycloheximide (CHX; 1 μ M). (B) Cells were fixed with 4% paraformaldehyde and used for cytochrome c immunocytochemistry. Nuclei were stained with H-33342 and correspond to the same field used for imaging cytochrome c staining. Neurons with released cytochrome c are indicated by arrows and neurons that entirely lost cytochrome c staining are indicated by arrowheads. The width of every scale bar corresponds to 30 μ m. (C) Individual neuronal somata marked by the boxes in (B) are shown at higher magnification (width = 10 μ m), cyt c, cytochrome c.

clei had lost cytochrome c staining, which suggested that, once released, cytochrome c was degraded in the cytoplasm. In the presence of zVAD-fmk (Figs. 6B and C, middle right panel), which prevented the appearance of all nuclear alterations, cytochrome c was released in many neurons. This suggested that zVAD-fmk-inhibitable caspases were involved primarily downstream of cytochrome c release to trigger chromatin condensation, but they were not responsible for the events leading to cytochrome c release in colchicine-treated CGC. We further tested whether

colchicine had any direct effect on mitochondrial loss of cytochrome c by exposing neurons in the presence of the translation inhibitor cycloheximide (CHX), which blocks apoptosis in this model (33) and acts upstream of mitochondria (49). No cytochrome c release from mitochondria was observed, even at later stages (20 hr, Figs. 6B and C, right panel) in this model system, although CHX did not prevent the initial colchicine-triggered microtubule breakdown. The results obtained by immunocytochemistry were confirmed fully by Western blots analysis of cytochrome c in both cytosolic and organelle fraction (Fig. 7). Taken together, these findings provided evidence that cytochrome c release occurred upstream of caspase activation and was triggered by cytoskeletal breakdown, but not by colchicine itself.

Modulation of Cell Death by Proteasome Inhibitors

We further investigated whether other proteases different from caspases would contribute to the delayed caspase-independent cell death. In many cases, CGC did not tolerate a prolonged incubation with several of the protease inhibitors tested. Thus, we added the various inhibitors 12 hr after the challenge with colchicine plus zVAD-fmk, at the time when cytochrome c release just began. Neuronal survival was then determined 18 hr later.

The highly selective and irreversible proteasome inhibitor *clasto*-lactacystin β -lactone (active lactacystin metabolite), in a concentration range from 10–20 μ M, reduced the percentage of condensed nuclei by 70% (Fig. 8). Similar effects were obtained with the proteasome inhibitor, MG 115 (z-Leu-Leu-Nva-CHO) in a concentration range from 1–20 μ M (Fig. 8). These proteasome inhibitors had only minor effects (less than 5% protection) on colchicine-induced apoptosis in the absence of zVAD-fmk, even when the inhibitors were added to the cultures together or prior to colchicine (not shown). The peptide aldehyde LLN-CHO (50–100 μ M) reduced cell

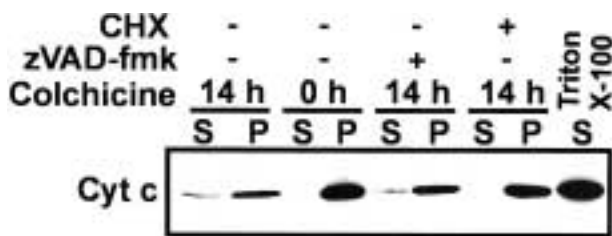


Fig. 7. Mitochondrial cytochrome c release is not prevented by caspase inhibition. Cytochrome c release into the cytosol (the cytosolic fraction is indicated by an S for supernatant) and the cytochrome c retained in the organelle fraction (indicated as P for pellet) were determined by Western blots. As control for maximal cytochrome c release, neurons were treated with 0.3% Triton X-100. CHX, cycloheximide; zVAD-fmk, N-benzyloxycarbonyl-Val-Ala-aspartyl-fluoromethyl ketone; cyt c, cytochrome c.

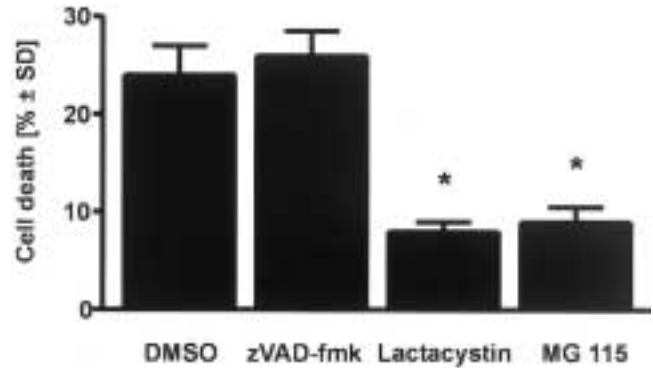


Fig. 8. Reduction of cell death by the proteasome inhibitors. Neurons were treated with colchicine (1 μ M) and N-benzyloxycarbonyl-Val-Ala-aspartyl-fluoromethyl ketone (zVAD-fmk; 100 μ M). After 12 hr incubation, solvent control dimethylsulfoxide (DMSO), additional zVAD-fmk (100 μ M), lactacystin (20 μ M), or N-benzyloxycarbonyl-Leu-Leu-Nva-aldehyde (MG 115; 5 μ M) were added for a further incubation time of 18 hr. After 30 hr, neurons were stained with H-33342 and cell death is expressed as percentage of nuclei with condensed chromatin. Data are mean values from triplicate determinations. * $p < 0.05$; solvent vs. proteasome inhibitors. SD, standard deviation.

death by 50% (not shown). Because LLN-CHO inhibited calpains as well as proteasome, we also tested the broad cysteine protease inhibitor, E 64 (1–40 μ M), which inhibited calpains and cathepsin B, H and L, the calpain inhibitor LLM-CHO (100–200 μ M), and the cathepsin B inhibitors CA074 (1–25 μ M) and zFK-tmK (1–10 μ M). None of these inhibitors significantly reduced cell death. Serine proteases inhibitors [N ^{α} -Tosyl-Lys-chlormethyl ketone (TLCK) and N ^{α} -Tosyl-Phe-chlormethyl ketone (TPCK)] the control peptide zF-cmk, or sequential additions of zVAD-fmk (Fig. 8) had no effect on cell demise. Altogether, these findings point at the proteasome as an important mediator of cell death in caspase-inhibited neurons.

Discussion

Neurons exposed to colchicine degenerated by a two-step mechanism: a caspase-independent loss of neurites followed by an apoptotic demise of neuronal somata. Caspase inhibition and Bcl-2 overexpression did not prevent neurite loss; whereas, they delayed the appearance of apoptosis. Most notably, caspase-inhibited neurons still died after a lag period of 24 hr, displaying key features of apoptosis, such as nuclear shrinkage, chromatin condensation, and DNA-fragmentation. In addition, neurons showed PS-exposure and mitochondrial permeabilization, which are often observed in apoptotic cells.

These findings contrast with the classical paradigm that the apoptotic morphology requires and results from activation of caspases alone (16,27). A dominant role of caspases in several models of

neuronal apoptosis is proven by the protective effects of viral caspase inhibitors (50,51) or peptide inhibitors (37,52–54). In vivo, caspase inhibition can significantly alleviate damage following cerebral ischemia (17,18), axotomy (55), head trauma (56), and intracerebral transplantation (57). Nevertheless, there is emerging evidence that inhibition of caspases does not always prevent apoptotic cell death. For instance, removal of the interdigital web and negative selection in the thymus occur independently of caspases (58,59). In vitro, cytolysis and mitochondrial membrane permeabilization has been observed, despite the presence of pan-caspase inhibitors, and although these compounds blocked oligonucleosomal DNA fragmentation and chromatin condensation in the same settings (60–63). In some cases, programmed cell death has been shown to occur without caspases being activated at all (64–66). A possible explanation for the contradictory results obtained with caspase inhibitors may be that this approach fails to rescue permanently from cell death when additional survival factors (i.e., neurotrophins) are lacking (25). The positive side of this consideration is that caspase inhibition in vivo eventually may buy sufficient time for injured cells to recover. The question, instead, arises as to whether pharmacological caspase inhibition may be an effective treatment in chronic neurodegenerative disease, when factors promoting regeneration are missing (26).

An additional question, which becomes relevant in molecular pathology, is whether caspase-independent cell death can have an apoptotic-like morphology. An increasing number of studies, including ours, suggest that this is possible (66–71). The delayed and caspase-independent cell death observed in the present study was characterized by typical apoptotic features, such as chromatin condensation (Fig. 3) and ordered DNA degradation (Fig. 4). In comparison to apoptosis induced by colchicine alone, where we observed chromatin condensation plus fragmentation to crescent-shaped patterns (Fig. 3), and degradation to large (Fig. 4) and oligonucleosomal DNA fragments (32), caspase-inhibited neurons seem to execute this part of the program only partially. Oligonucleosomal DNA fragmentation involves primarily the caspases-mediated activation of cytoplasmic nucleases (72) and it is clearly not featured in caspase-inhibited neurons. PS translocation, the most conspicuous plasma membrane event occurring in apoptosis can result from caspase activation (73), but it also can be mediated by alternative mechanisms (74). Regardless of the triggering event, the appearance of PS on the surface of neurons dying in the presence of caspase inhibitors (Fig. 5) suggests that they still would be recognized by phagocytes in vivo.

Mitochondrial dysfunction in apoptosis results in the release of pro-apoptotic factors, including caspases (75), cytochrome c (76), and the apoptosis-inducing factor (AIF) (77) from the intermembrane

space to the cytoplasm. In addition, loss of respiratory functions and ATP depletion may follow the irreversible opening of the permeability transition pore (78) and/or the loss of cytochrome c. The translocation of cytochrome c to the cytoplasm couples the mitochondrial cell death sensor to the activation of caspases. In colchicine-induced apoptosis, loss of the mitochondrial membrane potential occurs upstream of caspase activation, since caspase inhibitors do not prevent the loss of $\Delta\Psi$ (data not shown). Similarly, cytochrome c release occurs in a caspase-independent manner (Figs. 6 and 7). In contrast, the translation inhibitor, CHX, blocks apoptosis (33) by a mechanism upstream of mitochondria. One possible explanation for the effect of CHX may be the suppression of gene induction involved in the multimerization and translocation of proapoptotic Bax to mitochondria, as shown in sympathetic neurons deprived of nerve growth factor (49).

The oncogene *bcl-2* can prevent caspase-dependent and -independent cell death (46,79,80), acting primarily on mitochondria (81). Nevertheless, neurite loss is not altered by overexpression of this oncogene. However, in neuronal cultures from Bcl-2-overexpressing mice, colchicine-induced caspase activation is temporarily suppressed (data not shown). Time course studies show that this protection was, in fact, only ephemeral, and caspase activity increases later to the same extent as in observed wild type neurons. The transient protection provided by Bcl-2 in both caspase-dependent and caspase-independent paradigms (Figs. 1B and C) suggests that the two modes of cell death may share one commitment point at the level of mitochondria. These findings also suggest the existence of essential death effectors other than caspases, but which are still controlled by Bcl-2. One candidate is the mitochondrial flavoprotein AIF, which can elicit apoptotic nuclear changes in a caspase-independent manner (82). Moreover, other protease families, such as calpains, cathepsins, and the proteasome and serine proteases have been implicated in apoptosis (83–86).

The essential conclusions of this work are based on the observation that the poly-caspase inhibitor zVAD-fmk completely inhibits execution caspases in these neurons (Fig. 2). Although the experimental evidence shows that all active caspases in this system are blocked by zVAD-fmk, we cannot exclude that a yet unknown caspase not sensitive to zVAD-fmk might mediate pro-apoptotic events. Whereas this seems unlikely to us, it appears more plausible that another protease family may produce the apoptotic-like features found in caspase-inhibited neurons. The available evidence allows the conclusion that the proteasome may take over the role of an execution system (Fig. 8). In other models, the proteasome system is involved critically in apoptosis, acting at a point upstream of caspase activation, for example, in cerebellar granule cells deprived of extracellular potassium (87), in sympathetic neurons

deprived of nerve growth factor (88), or in T cells treated with glucocorticoids (85). However, inhibiting the proteasome does not modify colchicine-induced caspase activation. Thus, our data suggest the existence of an alternative pathway, as recently observed in other systems (68).

Our cell culture system models a situation where caspase inhibition may save time for the recovery of neurons in stress situations. If this does not occur, then other proteases may take over the execution to prevent the persistence of damaged cells. This suggests that: (1) the finding of neurons dying in vivo with apoptotic features does not always imply that caspase activation is causally involved in neuronal demise; and (2) that treatment of neurodegenerative disease solely with caspase inhibitors may not always be the most efficient way to rescue neurons. The combined use of caspase inhibitors with treatments aimed to foster active regeneration of sublethally injured neurons may be the most effective therapeutic approach (26).

Acknowledgement

The excellent technical assistance of M. Häberlin, N. Fehrenbacher, H. Naumann, and T. Schmitz is gratefully acknowledged. We are grateful to Dr. J.-C. Martinou (Geneva, Switzerland) for providing Bcl-2 transgenic mice, to Dr. P. Vandenabeele (Gent, Belgium) for providing recombinant caspase-2, and to Dr. F.O. Fackelmayer (Konstanz, Germany) for providing recombinant caspase-3. The Land Baden-Württemberg, the DFG grants We686/18-1, Ni519/1-1, and Ni519/2-1, and the EEC grants BMH4CT97-2410 and 12029-97-06 F1ED ISP D supported this study.

References

- Kerr JF, Wyllie AH, Currie AR. (1972) Apoptosis: a basic biological phenomenon with wide-ranging implications in tissue kinetics. *Br. J. Cancer* **26**: 239–257.
- Wyllie AH, Kerr JF, Currie AR. (1980) Cell death: the significance of apoptosis. *Int. Rev. Cytol.* **68**: 251–306.
- Raff MC. (1992) Social controls on cell survival and cell death. *Nature* **356**: 397–400.
- Oppenheim RW, Schwartz LM, Shatz CJ. (1992) Neuronal death, a tradition of dying. *J. Neurobiol.* **23**: 1111–1115.
- Leist M, Nicotera P. (1998) Apoptosis, excitotoxicity, and neuropathology. *Exp. Cell Res.* **239**: 183–201.
- Nicotera P, Leist M, Fava E, Berliocchi L, Volbracht C. (2000) Energy requirement for caspase activation and neuronal cell death. *Brain Pathol.* **10**: 276–282.
- Stefanis L, Burke RE, Greene LA. (1997) Apoptosis in neurodegenerative disorders. *Curr. Opin. Neurol.* **10**: 299–305.
- Mucke L, Masliah E, Yu GQ, et al. (2000) High-level neuronal expression of A β 1–42 in wild-type human amyloid protein precursor transgenic mice: synaptotoxicity without plaque formation. *J. Neurosci.* **20**: 4050–4058.
- Murphy KP, Carter RJ, Lione LA, et al. (2000) Abnormal synaptic plasticity and impaired spatial cognition in mice transgenic for exon 1 of the human Huntington's disease mutation. *J. Neurosci.* **20**: 5115–5123.
- Yamamoto A, Lucas JJ, Hen R. (2000) Reversal of neuropathology and motor dysfunction in a conditional model of Huntington's disease. *Cell* **101**: 57–66.
- Braak E, Braak H, Mandelkow EM. (1994) A sequence of cytoskeleton changes related to the formation of neurofibrillary tangles and neuropil threads. *Acta Neuropathol.* **87**: 554–567.
- Johnson EM, Deckwerth TL. (1993) Molecular mechanisms of developmental neuronal death. *Annu. Rev. Neurosci.* **16**: 31–46.
- Bibb JA, Yan Z, Svenningsson P, et al. (2000) Severe deficiencies in dopamine signaling in presymptomatic Huntington's disease mice. *Proc. Natl. Acad. Sci. USA* **97**: 6809–6814.
- Carter RJ, Lione LA, Humby T, et al. (1999) Characterization of progressive motor deficits in mice transgenic for the human Huntington's disease mutation. *J. Neurosci.* **19**: 3248–3257.
- Chapman PF, White GL, Jones MW, et al. (1999) Impaired synaptic plasticity and learning in aged amyloid precursor protein transgenic mice. *Nat. Neurosci.* **2**: 271–276.
- Nicholson DW. (1999) Caspase structure, proteolytic substrates, and function during apoptotic cell death. *Cell Death Differ.* **6**: 1028–1042.
- Hara H, Friedlander RM, Gagliardini V, et al. (1997) Inhibition of interleukin 1 β converting enzyme family proteases reduces ischemic and excitotoxic neuronal damage. *Proc. Natl. Acad. Sci. USA* **94**: 2007–2012.
- Loddick SA, MacKenzie A, Rothwell NJ. (1996) An ICE inhibitor, z-VAD-DCB attenuates ischaemic brain damage in the rat. *Neuroreport* **7**: 1465–1468.
- Li M, Ona VO, Guegan C, et al. (2000) Functional role of caspase-1 and caspase-3 in an ALS transgenic mouse model. *Science* **288**: 335–339.
- Ona VO, Li M, Vonsattel JP, et al. (1999) Inhibition of caspase-1 slows disease progression in a mouse model of Huntington's disease. *Nature* **399**: 263–267.
- Johnson MD, Xiang H, London S, et al. (1998) Evidence for involvement of Bax and p53, but not caspases, in radiation-induced cell death of cultured postnatal hippocampal neurons. *J. Neurosci. Res.* **54**: 721–733.
- Stefanis L, Park DS, Friedman WJ, Greene LA. (1999) Caspase-dependent and -independent death of camptothecin-treated embryonic cortical neurons. *J. Neurosci.* **19**: 6235–6247.
- Miller TM, Moulder KL, Knudson CM, et al. (1997) Bax deletion further orders the cell death pathway in cerebellar granule cells and suggests a caspase-independent pathway to cell death. *J. Cell Biol.* **139**: 205–217.
- Selznick LA, Zheng TS, Flavell RA, Rakic P, Roth KA. (2000) Amyloid β -induced neuronal death is bax-dependent but caspase-independent. *J. Neuropathol. Exp. Neurol.* **59**: 271–279.
- Deshmukh M, Vasilakos J, Deckwerth TL, Lampe PA, Shivers BD, Johnson EM. (1996) Genetic and metabolic status of NGF-deprived sympathetic neurons saved by an inhibitor of ICE family proteases. *J. Cell Biol.* **135**: 1341–1354.
- Deshmukh M, Kuida K, Johnson EM. (2000) Caspase inhibition extends the commitment to neuronal death beyond cytochrome c release to the point of mitochondrial depolarization. *J. Cell Biol.* **150**: 131–143.
- Samali A, Zhivotovsky B, Jones D, Nagata S, Orrenius S. (1999) Apoptosis: cell death defined by caspase activation. *Cell Death Differ.* **6**: 495–496.
- Leist M, Single B, Castoldi AF, Kühnle S, Nicotera P. (1997) Intracellular adenosine triphosphate (ATP) concentration: a switch in the decision between apoptosis and necrosis. *J. Exp. Med.* **185**: 1481–1486.
- Nicotera P, Leist M, Manzo L. (1999) Neuronal cell death: a demise with different shapes. *Trends Pharmacol. Sci.* **20**: 46–51.
- Mattson MP, Keller JN, Begley JG. (1998) Evidence for synaptic apoptosis. *Exp. Neurol.* **153**: 35–48.
- Finn JT, Weil M, Archer F, Siman R, Srinivasan A, Raff MC. (2000) Evidence that Wallerian degeneration and localized axon degeneration induced by local neurotrophin deprivation do not involve caspases. *J. Neurosci.* **20**: 1333–1341.
- Bonfoco E, Ceccatelli S, Manzo L, Nicotera P. (1995) Colchicine induces apoptosis in cerebellar granule cells. *Exp. Cell Res.* **218**: 189–200.

33. Volbracht C, Leist M, Nicotera P. (1999) ATP controls neuronal apoptosis triggered by microtubule breakdown or potassium deprivation. *Mol. Med.* **5**: 477–489.
34. Martinou JC, Dubois-Dauphin M, Staple JK, et al. (1994) Overexpression of BCL-2 in transgenic mice protects neurons from naturally occurring cell death and experimental ischemia. *Neuron* **13**: 1017–1030.
35. Leist M, Volbracht C, Fava E, Nicotera P. (1998) 1-methyl-4-phenylpyridinium induces autocrine excitotoxicity, protease activation, and Neuronal apoptosis. *Mol. Pharmacol.* **54**: 789–801.
36. Single B, Leist M, Nicotera P. (1998) Simultaneous release of adenylate kinase and cytochrome c in cell death. *Cell Death Differ.* **5**: 1001–1003.
37. Leist M, Volbracht C, Kühnle S, Fava E, Ferrando-May E, Nicotera P. (1997) Caspase-mediated apoptosis in Neuronal excitotoxicity triggered by nitric oxide. *Mol. Med.* **3**: 750–764.
38. Van de Craen M, Vandenaabeele P, Declercq W, et al. (1997) Characterization of seven murine caspase family members. *FEBS Lett.* **403**: 61–69.
39. Kipp M, Schwab BL, Przybylski M, Nicotera P, Fackelmayer FO. (2000) Apoptotic cleavage of scaffold attachment factor A (SAF-A) by caspase-3 occurs at a noncanonical cleavage site. *J. Biol. Chem.* **275**: 5031–5036.
40. Leist M, Single B, Künstle G, Volbracht C, Hentze H, Nicotera P. (1997) Apoptosis in the absence of poly-(ADP-ribose) polymerase. *Biochem. Biophys. Res. Commun.* **233**: 518–522.
41. Talanian RV, Quinlan C, Trautz S, et al. (1997) Substrate specificities of caspase family proteases. *J. Biol. Chem.* **272**: 9677–9682.
42. Thornberry NA. (1994) Interleukin-1 β converting enzyme. *Methods Enzymol.* **244**: 615–631.
43. Garcia-Calvo M, Peterson EP, Rasper DM, et al. (1999) Purification and catalytic properties of human caspase family members. *Cell Death Differ.* **6**: 362–369.
44. Haldar S, Basu A, Croce CM. (1997) Bcl2 is the guardian of microtubule integrity. *Cancer Res.* **57**: 229–233.
45. Green DR, Reed JC. (1998) Mitochondria and apoptosis. *Science* **281**: 1309–1312.
46. Haraguchi M, Torii S, Matsuzawa S, et al. (2000) Apoptotic protease activating factor 1 (Apaf-1)-independent cell death suppression by bcl-2. *J. Exp. Med.* **191**: 1709–1720.
47. Garcia-Calvo M, Peterson EP, Leiting B, Ruel R, Nicholson DW, Thornberry NA. (1998) Inhibition of human caspases by peptide-based and macromolecular inhibitors. *J. Biol. Chem.* **273**: 32608–32613.
48. Troy CM, Rabacchi SA, Friedman WJ, Frappier TF, Brown K, Shelanski ML. (2000) Caspase-2 mediates Neuronal cell death induced by β -amyloid. *J. Neurosci.* **20**: 1386–1392.
49. Putcha GV, Deshmukh M, Johnson EM. (2000) Inhibition of apoptotic signaling cascades causes loss of trophic factor dependence during Neuronal maturation. *J. Cell. Biol.* **149**: 1011–1018.
50. Gagliardini V, Fernandez PA, Lee RK, et al. (1994) Prevention of vertebrate Neuronal death by the crmA gene. *Science* **263**: 826–828.
51. Enari M, Hug H, Nagata S. (1995) Involvement of an ICE-like protease in Fas-mediated apoptosis. *Nature* **375**: 78–81.
52. Milligan CE, Prevet D, Yaginuma H, et al. (1995) Peptide inhibitors of the ICE protease family arrest programmed cell death of motoneurons in vivo and in vitro. *Neuron* **15**: 385–393.
53. Stefanis L, Park DS, Yan CY, et al. (1996) Induction of CPP32-like activity in PC12 cells by withdrawal of trophic support. Dissociation from apoptosis. *J. Biol. Chem.* **271**: 30663–30671.
54. Troy CM, Stefanis L, Prochiantz A, Greene LA, Shelanski ML. (1996) The contrasting roles of ICE family proteases and interleukin-1 β in apoptosis induced by trophic factor withdrawal and by copper/zinc superoxide dismutase down-regulation. *Proc. Natl. Acad. Sci. USA* **93**: 5635–5640.
55. de Bilbao F, Dubois-Dauphin M. (1996) Acute application of an interleukin-1 β -converting enzyme-specific inhibitor delays axotomy-induced motoneurone death. *Neuroreport* **7**: 3051–3054.
56. Yakovlev AG, Knoblach SM, Fan L, Fox GB, Goodnight R, Faden AI. (1997) Activation of CPP32-like caspases contributes to Neuronal apoptosis and neurological dysfunction after traumatic brain injury. *J. Neurosci.* **17**: 7415–7424.
57. Schierle GS, Hansson O, Leist M, Nicotera P, Widner H, Brundin P. (1999) Caspase inhibition reduces apoptosis and increases survival of nigral transplants. *Nat. Med.* **5**: 97–100.
58. Doerfler P, Forbush KA, Perlmutter RM. (2000) Caspase enzyme activity is not essential for apoptosis during thymocyte development. *J. Immunol.* **164**: 4071–4079.
59. Chautan M, Chazal G, Cecconi F, Gruss P, Golstein P. (1999) Interdigital cell death can occur through a necrotic and caspase-independent pathway. *Curr. Biol.* **9**: 967–970.
60. Amarante-Mendes GP, Finucane DM, Martin SJ, Cotter TG, Salvesen GS, Green DR. (1998) Anti-apoptotic oncogenes prevent caspase-dependent and independent commitment for cell death. *Cell Death Differ.* **5**: 298–306.
61. Hirsch T, Marchetti P, Susin SA, et al. (1997) The apoptosis-necrosis paradox. Apoptogenic proteases activated after mitochondrial permeability transition determine the mode of cell death. *Oncogene* **15**: 1573–1581.
62. Sarin A, Williams MS, Alexander-Miller MA, Berzofsky JA, Zacharchuk CM, Henkart PA. (1997) Target cell lysis by CTL granule exocytosis is independent of ICE/Ced-3 family proteases. *Immunity* **6**: 209–215.
63. Trapani JA, Jans DA, Jans PJ, Smyth MJ, Browne KA, Sutton VR. (1998) Efficient nuclear targeting of granzyme B and the nuclear consequences of apoptosis induced by granzyme B and perforin are caspase-dependent, but cell death is caspase-independent. *J. Biol. Chem.* **273**: 27934–27938.
64. Chi S, Kitanaka C, Noguchi K, et al. (1999) Oncogenic Ras triggers cell suicide through the activation of a caspase-independent cell death program in human cancer cells. *Oncogene* **18**: 2281–2290.
65. Kawahara A, Ohsawa Y, Matsumura H, Uchiyama Y, Nagata S. (1998) Caspase-independent cell killing by Fas-associated protein with death domain. *J. Cell. Biol.* **143**: 1353–1360.
66. Nylansted J, Rohde M, Brand K, Bastholm L, Elling F, Jäättelä M. (2000) Inhibition of Hsp70 synthesis activates a novel caspase-independent and Bcl-2 resistant death pathway in breast cancer cells. *Proc. Natl. Acad. Sci. USA* **97**: 7871–7876.
67. McCarthy NJ, Whyte MK, Gilbert CS, Evan GI. (1997) Inhibition of Ced-3/ICE-related proteases does not prevent cell death induced by oncogenes, DNA damage, or the Bcl-2 homologue Bak. *J. Cell. Biol.* **136**: 215–227.
68. Monney L, Otter I, Olivier R, et al. (1998) Defects in the ubiquitin pathway induce caspase-independent apoptosis blocked by Bcl-2. *J. Biol. Chem.* **273**: 6121–6131.
69. Brunet CL, Gunby RH, Benson RS, Hickman JA, Watson AJ, Brady G. (1998) Commitment to cell death measured by loss of clonogenicity is separable from the appearance of apoptotic markers. *Cell Death Differ.* **5**: 107–115.
70. Déas O, Dumont C, MacFarlane M, et al. (1998) Caspase-independent cell death induced by anti-CD2 or staurosporine in activated human peripheral T lymphocytes. *J. Immunol.* **161**: 3375–3383.
71. Xiang J, Chao DT, Korsmeyer SJ. (1996) BAX-induced cell death may not require interleukin 1 β -converting enzyme-like proteases. *Proc. Natl. Acad. Sci. USA* **93**: 14559–14563.
72. Enari M, Sakahira H, Yokoyama H, Okawa K, Iwamatsu A, Nagata S. (1998) A caspase-activated DNase that degrades DNA during apoptosis, and its inhibitor ICAD. *Nature* **391**: 43–50.
73. Martin SJ, Finucane DM, Amarante-Mendes GP, O'Brien GA, Green DR. (1996) Phosphatidylserine externalization during CD95-induced apoptosis of cells and cytoplasts requires ICE/CED-3 protease activity. *J. Biol. Chem.* **271**: 28753–28756.
74. Hirt UA, Gantner F, Leist M. (2000) Phagocytosis of non-apoptotic cells dying by caspase-independent mechanisms. *J. Immunol.* **164**: 6520–6529.

75. Susin SA, Lorenzo HK, Zamzami N, et al. (1999) Mitochondrial release of caspase-2 and -9 during the apoptotic process. *J. Exp. Med.* **189**: 381–394.
76. Liu X, Kim CN, Yang J, Jemmerson R, Wang X. (1996) Induction of apoptotic program in cell-free extracts: requirement for dATP and cytochrome c. *Cell* **86**: 147–157.
77. Susin SA, Zamzami N, Castedo M, et al. (1996) Bcl-2 inhibits the mitochondrial release of an apoptogenic protease. *J. Exp. Med.* **184**: 1331–1341.
78. Bernardi P, Colonna R, Costantini P, et al. (1998) The mitochondrial permeability transition. *Biofactors* **8**: 273–281.
79. Tsujimoto Y, Shimizu S, Eguchi Y, Kamiike W, Matsuda H. (1997) Bcl-2 and Bcl-xL block apoptosis as well as necrosis: possible involvement of common mediators in apoptotic and necrotic signal transduction pathways. *Leukemia* **11**: 380–382.
80. Kane DJ, Ord T, Anton R, Bredesen DE. (1995) Expression of bcl-2 inhibits necrotic neural Cell death. *J. Neurosci. Res.* **40**: 269–275.
81. Kroemer G, Reed JC. (2000) Mitochondrial control of Cell death. *Nat. Med.* **6**: 513–519.
82. Susin SA, Lorenzo HK, Zamzami N, et al. (1999) Molecular characterization of mitochondrial apoptosis-inducing factor. *Nature* **397**: 441–446.
83. Squier MK, Miller AC, Malkinson AM, Cohen JJ. (1994) Calpain activation in apoptosis. *J. Cell. Physiol.* **159**: 229–237.
84. Deiss LP, Galinka H, Berissi H, Cohen O, Kimchi A. (1996) Cathepsin D protease mediates programmed Cell death induced by interferon- γ , Fas/APO-1 and TNF- α . *Embo J.* **15**: 3861–3870.
85. Grimm LM, Goldberg AL, Poirier GG, Schwartz LM, Osborne BA. (1996) Proteasomes play an essential role in thymocyte apoptosis. *Embo J.* **15**: 3835–3844.
86. Wright SC, Schellenberger U, Wang H, Kinder DH, Talhouk JW, Larrick JW. (1997) Activation of CPP32-like proteases is not sufficient to trigger apoptosis: inhibition of apoptosis by agents that suppress activation of AP24, but not CPP32-like activity. *J. Exp. Med.* **186**: 1107–1117.
87. Canu N, Barbato C, Ciotti MT, Serafino A, Dus L, Calissano P. (2000) Proteasome involvement and accumulation of ubiquitinated proteins in cerebellar granule neurons undergoing apoptosis. *J. Neurosci.* **20**: 589–599.
88. Sadoul R, Fernandez PA, Quiquerez AL, et al. (1996) Involvement of the proteasome in the programmed Cell death of NGF-deprived sympathetic neurons. *Embo J.* **15**: 3845–3852.